SALTS AND RADIATION PRODUCTS ON THE SURFACE OF EUROPA

M.E. Brown

Division of Geological and Planetary Sciences, California Institute of Technology, Pasadena, CA 91125

K.P. Hand

Jet Propulsion Laboratory, California Institute of Technology, Pasadena, CA 91109
Draft version March 1, 2013

ABSTRACT

The surface of Europa could contain the compositional imprint of a underlying interior ocean, but competing hypotheses differ over whether spectral observations from the Galileo spacecraft show the signature of ocean evaporates or simply surface radiation products unrelated to the interior. Using adaptive optics at the W.M. Keck Observatory, we have obtained spatially resolved spectra of most of the disk of Europa at a spectral resolution ~ 40 times higher than seen by the Galileo spacecraft. These spectra show a previously undetected distinct signature of magnesium sulfate salts on Europa, but the magnesium sulfate is confined to the trailing hemisphere and spatially correlated with the presence of radiation products like sulfuric acid and SO_2. On the leading, less irradiated, hemisphere, our observations rule out the presence of many of the proposed sulfate salts, but do show the presence of distorted water ice bands. Based on the association of the potential $MgSO_4$ detection on the trailing side with other radiation products, we conclude that $MgSO_4$ is also a radiation product, rather than a constituent of a Europa ocean brine. Based on ocean chemistry models, we hypothesize that, prior to irradiation, magnesium is primarily in the form of $MgCl_2$, and we predict that NaCl and KCl are even more abundant, and, in fact, dominate the non-ice component of the leading hemisphere. We propose observational tests of this new hypothesis.

Subject headings: Planets and satellites: Europa – Planets and satellites: composition – Planets and satellites: surfaces

1. INTRODUCTION

Jupiter's moon Europa may harbor a global salty liquid water ocean of ~ 100 km in depth and 2-3 times the volume of all the liquid water on Earth (Anderson et al. 1998; Kivelson et al. 2000; Zimmer et al. 2000). This liquid water, in combination with a rocky silicate sea floor and radiolytically produced surface oxidants, may provide for a chemically rich ocean that would be considered habitable by terrestrial standards (Chyba 2000; Hand et al. 2009). While the surface of Europa might contain important clues about the composition of an interior ocean, after almost a decade of scrutiny from the Galileo spacecraft, debate still persists about the nature of the surface chemistry and the relative roles of exogenous radiation processing versus endogenous oceanic emplacement. From the current data, Europa can be viewed as a purely passive ice shell onto which ion and electron bombardment create a limited chemical cycle confined to a thin surface layer, or it can be seen as a geologically active body with a chemically rich ocean that leaves a compositional fingerprint on the surface ice.

One key to understanding the nature of Europa is determining whether the composition of the icy surface reflects the interior ocean chemistry. Early spectroscopy results from the NIMS (Near Infrared Mapping Spectrograph) (Carlson et al. 1992) instrument on the Galileo spacecraft suggested that the surface of Europa was dominated by hydrated sulfate salts of the sort that would be expected in evaporates from an internal ocean (McCord

et al. 1998). The finding that these spectral signatures are more prevalent in what appear to be younger terrains bolsters the hypothesis that these are more-recently emplaced evaporates (McCord et al. 2001). Further study of the spectra, however, showed that these same NIMS surface spectra could be explained equally well by a surface dominated by hydrated sulfuric acid (Carlson et al. 1999). Sulfuric acid is an expected product of the bombardment of an icy surface with sulfur ions (Carlson et al. 2002; Strazzulla et al. 2007). At Europa these sulfur ions are ultimately derived from molecules such as SO_2 released from volcanoes on Io and subsequently dissociated, ionized, and accelerated by Jupiters rapidly spinning magnetic field until they impact Europa. Such radiolysis could also explain the SO_2 (Lane et al. 1981) and sulfur allotropes (Carlson et al. 2009) seen on the surface of Europa and their preferential appearance on the more heavily bombarded trailing hemisphere (Paranicas et al. 2001, 2002). The presence of sulfuric acid and additional sulfur products on the surface of Europa appears nearly inescapable, yet the salt hypothesis also remains compelling.

Over the past decade, considerable work has gone into detailed modeling of individual surface units on Europa and developing a combined picture where hydrated sulfuric acid indeed dominates the trailing hemisphere, but hydrated salts of various compositions are more dominant elsewhere (Dalton et al. 2005; Dalton 2007; Shirley et al. 2010; Dalton et al. 2012a,b). This analysis relies on attempting to fit the observed NIMS spectra by linearly combining spectral components from a library composed

of laboratory spectra of hydrated salts, hydrated sulfuric acid, and water ice. Unfortunately, the NIMS spectra are at a sufficiently low spectral resolution that no distinct spectral features that would uniquely identify any of the non-ice spectral components are visible. Instead, the fit is largely determined by the broad shapes of the distorted water bands. A careful examination of even the most salt-rich modeled spectra suggests that simple intimate mixtures of hydrated sulfuric acid and water ice are capable of providing satisfactory fits to the data (Carlson et al. 2005). While both the hydrated salt and sulfuric acid hypotheses are compelling, we find, in agreement with McCord et al. (2010), that the NIMS data provides too low of a spectral resolution to discriminate between these current hypotheses or provide alternatives. Higher spectral resolution data has been obtained from ground-based telescopes, but, in general, these spectra cover an entire hemisphere of Europa, so icy and non-icy regions of the surface cannot be spatially discriminated (Calvin et al. 1995).

Modern infrared spectrographs coupled with adaptive optics systems on large ground based telescopes have both the spatial and spectral resolution required to potentially answer the question of the composition of the non-ice material on Europa. An early observation of the trailing hemisphere of Europa using adaptive optics at the W.M. Keck observatory (Spencer et al. 2006) showed no conclusive spectral features in the 1.50-1.75 μm wavelength region where many of the proposed salts should have spectral absorptions, suggesting that pure hydrated salts are not dominant on the trailing hemisphere, but with the limited spatial coverage and limited spectral band, many additional explanations are possible.

In order to continue the investigation of the composition of the surface of Europa at higher spectral resolution, we obtained high resolution spatially resolved spectra of Europa in wavelength regions between 1.4 and 2.4 μm using the adaptive optics system and the OSIRIS integral field spectrograph at the W.M. Keck Observatory (Larkin et al. 2003). Here we report on these new observations, discuss a new spectral feature discovered on the trailing hemisphere at this resolution, and suggest a possible identification of the species responsible and a scenario plausibly explaining the species and its spatial distribution.

2. OBSERVATIONS AND DATA REDUCTION

We observe Europa on the nights of 18, 19, and 20 September 2011 (UT), covering nearly all Europa longitudes. In the setup used, OSIRIS obtained a simultaneous spectrum at each of 1024 spatially resolved points within a 0.56 by 2.24 arcsecond region of the sky at a pixel scale of 0.035 by 0.035 acrseconds. At the time of observation, Europa had an angular diameter on the sky of 1.028 arcseconds, so the full disk of Europa could be covered in two pointings. We used both the broad band H and K band settings to cover wavelength ranges of 1.473 - 1.803 μm (Hbb setting) and 1.956 - 2.381 μm (Kbb setting), respectively. For each spectral setting we first observed half of Europa's disk, offset the telescope 20 arcseconds north to record a spectrum of the sky, and then offset back to the other half of Europa's disk. Solar type stars were observed at each spectral setting in order to calibrate telluric absorption and to construct a relative

reflectance spectrum (see Table 1 for observational details). The raw OSIRIS data were turned into a spectral data cube through the thoroughly automated OSIRIS DRP (data reduction package) that includes data extraction, calibration, and precise mosaicing. Because of the large range of air masses through which Europa and the calibrator stars were observed, we found that a single telluric absorption calibration correction was insufficient for both halves of a pair of Europa observations. We thus interrupted the DRP at the calibration step and manually corrected for telluric absorption. We first divided the spectrum by the spectrum of a solar-type telluric calibrator that was observed as close in airmass as possible. We further corrected these spectra by constructing a transmission function by dividing spectra of the same star taken at two different airmasses and dividing the spectrum of Europa by an exponentially scaled version of this transmission function. The scaling was found empirically for each individual observation. Because each observation included hundreds of individual spectra, the scaling and thus the transmission correction could be found to extremely high precision. In addition, we found that the DRP is not optimized for the extraction of precision spectra of continuum sources such as Europa. In particular, small scale spectral variations appeared that were correlated with location on the spectral format on each of the observations. To correct these, we implemented a separate calibration step where we combined spectra of a calibration star to fill the entrance aperture. We then extracted these spatially resolved spectra, which should be identical at each spatial position. We constructed a spatial-spectral flat-field map to normalize the spectra so they are identical. We then used this flat-field map to correct the Europa and the Europa calibration star spectra. After this additional step, no spatially correlated spectral features were observable in the extracted spectra of Europa. The final data product consists of a single data cube for each night at each setting (2 cubes were obtained for each setting on 19 September) with full wavelength and relative reflectance calibration of the spectrum at each point. Over the three night period, we were able to obtain spectra at a spatial resolution of ~150 km over nearly the entire surface of Europa at a spectral resolution approximately 40 times higher than that of the NIMS instrument on Galileo.

3. SPECTRAL MAPS

As a first step to studying the surface composition, we generated a global map of the non-water ice material across the surface of Europa. Several model-dependent methods have been used in an attempt to map the abundance of the non-ice material on the surface of Europa (McCord et al. 1999; Carlson et al. 1999; Grundy et al. 2007). We note that the general features of all of these methods is reproduced by making the simple observation that a distinguishing characteristic between the icy and non-icy material is the depth of the water ice absorption feature at 2 μm. We measure the depth of the 2 μm water absorption feature at each spatial point by taking a median of the reflectance between 2.198 μm and 2.245 μm and dividing by the median of the reflectance between 1.990 μm and 2.040 μm. Maps of the value of this ratio are created for each of three nights of observation, and the maps are projected to a cylindrical projection using
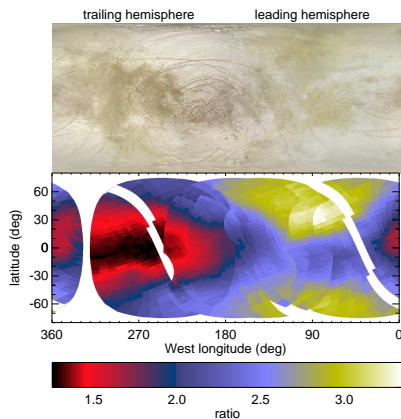
FIG. 1.— The Voyager color base map of Europa compared to a cylindrically projected map of the ratio of the albedo at 2.2 μm to that at 2.0 μm, a proxy for the fractional contribution of water ice. This map reproduces the well-known result that the orbitally trailing side of Europa (centered at a longitude of 270°) contains the least pure water ice, while the higher latitude regions host the most pure ice. These data are the first to cover the complete leading hemisphere (centered at a longitude of 90°), and show that this hemisphere, too, has less-pure ice than the poles.
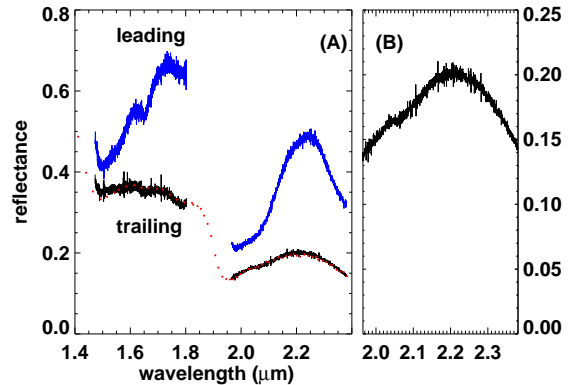

FIG. 2.— (A) Representative reflectance spectra from the surface of Europa, including from the low latitude dark trailing side (black), the low latitude bright leading side (blue). Uncertainty in the spectra can be seen from the scatter of the individual points. The red dots show the spectrum measured by NIMS from approximately the same region as our trailing side spectrum (Dalton 2007), showing the good agreement with our spectrum. (B) An enlargement of the region of the trailing hemisphere spectrum showing the distinct 2.07 μm absorption feature.

the mapping tools in the IDL software package. In regions of overlapping coverage between the three nights, the average value is used. The resulting ratio images (Fig. 1), reproduce the basic features seen in previous maps. The low latitude trailing hemisphere contains the largest fraction of non-water ice material. The high latitude regions contain the most pure water ice. The low latitude leading hemisphere – which had never been fully mapped before – also contains a significant abundance of non-water-ice material, though the amount is less than on the trailing hemisphere, and the overall reflectance of this hemisphere is higher.

To study the composition of the surface materials on Europa, we extract spectra from two areas of the satellite: the dark low latitude trailing hemisphere with the highest fraction of non-water ice material (where the 2.2 to 2.0 μm ratio is less than 1.3) and the bright low latitude leading hemisphere (with a ratio of less than 2.18) (Fig. 2). No calibration is available to turn these relative reflectance spectra into absolute reflectances. We estimate the absolute reflectances for each spectral data cube, however, by taking a mean of all spectra from the surface of Europa and comparing to full-disk spectra of Europa previously calibrated by standard methods (Calvin et al. 1995). We anticipate that the absolute reflectance calibration is precise to approximately 10%. The relative calibration between spatial locations and spectral settings should be significantly more precise.

The spectra are in good agreement with the lower resolution NIMS data obtained by the Galileo spacecraft on each of these general regions (Fig. 2), and, in general, at the higher resolution of the OSIRIS spectra little additional spectral detail is apparent. The most prominent exception, however, is the previously unobserved high resolution spectrum of the dark material on the trailing side of Europa. At the higher spectral resolution of our current data, the dark trailing side contains a clear

spectral absorption feature at 2.07 μm that was not detectable by NIMS. The 2.07 μm absorption feature appears in the trailing hemisphere equatorial spectra, but not in the simultaneously obtained polar spectra of the trailing hemisphere, confirming that the feature is real and not a function of the (identical) data reduction and calibration.

The appearance of the 2.07 μm feature on the trailing hemisphere and its non-appearance on the leading hemisphere suggests that it might be related to the strong trailing hemisphere irradiation. To explore this hypothesis, we create a spatial map of the strength of the 2.07 μm absorption. We define the continuum in the 2.07 μm region by fitting line segments to the region between 1.97 and 2.04 μm and between 2.10 and 2.18 μm and taking the point closest to the data of the two line segments at each wavelength as the continuum. We measure the strength of the absorption by integrating the line absorption from 2.035 to 2.100 μm, and show a spatial map of the absorption strength in Fig. 3. This method is crude but gives a simple continuum definition which is continuous across different types of spectra ranging from concave up on the trailing hemisphere to concave down on the leading hemisphere. The precise definition of this continuum level is uncertain, so the uncertainty in measuring the strength of this absorption is moderately high, but the absorption feature nonetheless appears primarily confined to the trailing hemisphere (Fig. 1). In fact, the 2.07 μm absorption feature appears well correlated with the locations of the trailing hemisphere non-water ice component and with the UV absorption seen in Voyager data that has been attributed to the presence of SO_2 – a radiation product – on the trailing hemisphere (Lane et al. 1981; McEwen 1986) It thus appears that the 2.07 μm absorption is strongly correlated with the presence of SO_2, a clue that the species causing this absorption is likely a radiolytic product. In the next section we attempt to identify this product.
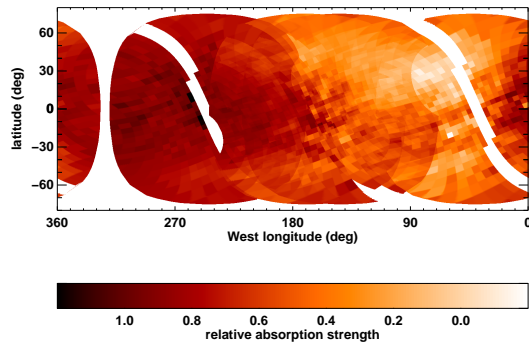
4. SPECTRAL IDENTIFICATION AND MODELING

FIG. 3.— A map of the strength of the 2.07 μm absorption. While defining the continuum level across the feature is difficult, particularly across the transition from the non-icy trailing hemisphere to the icier leading hemisphere, the map nonetheless suggests that the species causing the 2.07 μm feature is predominantly located on the trailing hemisphere, similar to known radiation products.

We search proposed radiolytic products for 2.07 μm absorption features. The primary products in the sulfur radiolytic cycle are sulfur allotropes, H_2SO_4, SO_2, S, and H_2S (Carlson et al. 2002; Moore et al. 2007). None of these has absorption features at or near 2.07 μm (Carlson et al. 2002; Fink & Sill 1982). Expanding our search beyond already proposed radiation products, we examined cryogenic spectral libraries (Dalton et al. 2005; Dalton 2007; Dalton & Pitman 2012), products from ice irradiation experiments (Hudson & Moore 2001; Moore et al. 2007, e.g.), and the full ASTER (Baldridge et al. 2009) and USGS (Clark et al. 2007) digital spectral libraries (though as an important caveat, the spectra in these two libraries are all obtained at room temperature, and subtle features like that here are known to change with temperature). While minerals with features near 2.07 μm can occasionally be found, in almost all cases there are stronger bands that would be predicted that are not observed. Of all of the spectra examined, an appropriate 2.07 μm absorption feature appears exclusively in some spectra of flash frozen $MgSO_4$ brines (Dalton et al. 2005; Orlando et al. 2005) (brines, in this context, refers to saturated solutions which are flash frozen and are thus not in a pure mineral form) and in measurements of the absorption coefficients of pure epsomite ($MgSO_4 \cdot 7H_2O$) (Dalton & Pitman 2012).

To expand our search, we obtained cryogenic laboratory spectra of a wide variety of potentially plausible materials, including $FeSO_4 \cdot H_2O$, $FeSO_4 \cdot 7H_2O$, MgS_4, $MgSO_4 \cdot 7H2O$, $CaSO_4 \cdot 0.5H_2O$, H_2SO_4, $(NH_4)2SO_4$, Na_2CO_3, $MgCO_3$, NH_4Cl, NaCl, KCl, NaSCN, NaOCl, $Mg(OH)_2$, NaOH, H_2O_2, CH_3OH, C_2H_5OH, NH_3, and CO_2. Samples were placed on gold target in small liquid nitrogen dewar with a nitrogen purge and spectra were collected with an Analytical Spectral Devices Field-Spec spectroradiometer covering the range from 0.35-2.5 μm, and with a MIDAC M4500 Fourier transform spectrometer covering the range from approximately 1.5-16 μm. Salts were examined in pure crystalline form and after dissolution in ultrapure deionized water. Addition-
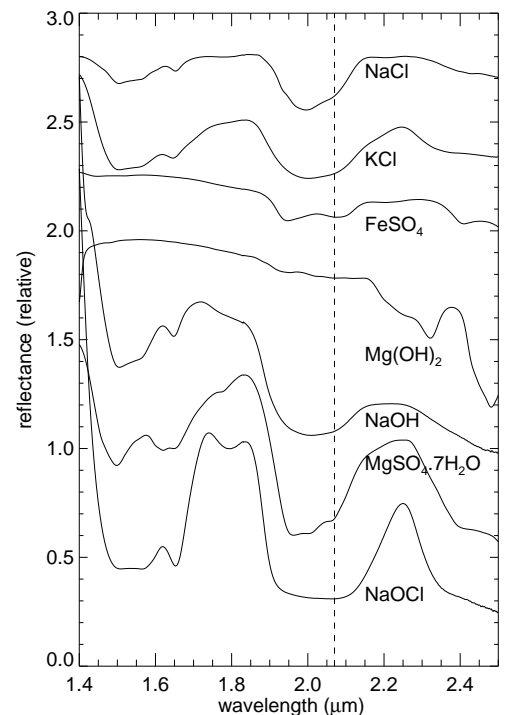

FIG. 4.— Example cryogenic laboratory spectra of frozen crushed brines and of epsomite. The spectra are scaled to unity at 1.8 μm and each spectrum is offset by 0.3 units from the spectrum below it. The location of the 2.07 μm absorption feature seen on the trailing hemisphere of Europa is shown for comparison. In these and all other spectra obtained, a 2.07 μm absorption feature was seen only for pure epsomite ($MgSO_4 \cdot 7H_2O$).

ally, salts and their crystalline brine forms were crushed, sieved and analyzed at 77 K with the above spectrometers for grain size fractions of < 63 μm, 63-106 μm, 106-180 μm, 180-300 μm, and 300-600 μm. Example spectra are shown in Fig. 4. Most spectra show no absorption features near the observed 2.07 μm region. The sole exception is epsomite ($MgSO_4 \cdot 7\,H_2O$), where we also detect the same 2.07 μm absorption feature seen in magnesium sulfate brines (Dalton et al. 2005; Orlando et al. 2005) and in previous laboratory spectra of epsomite (Dalton & Pitman 2012).

Magnesium sulfate brine, water ice, and hydrated sulfuric acid are components of the Dalton et al. spectral libraries, so we experiment with the linear combination analysis as performed in Dalton (2007) and subsequent papers. As a check of the spectral library and the method, we first model all of the spectra from Dalton (2007) and Shirley et al. (2010) and find that we recover the same fractional mineral abundances within a few percent. We next turn to modeling our spectrum of the equatorial region of the trailing hemisphere. Our χ^2 minimization finds that the best fit to this spectrum is composed nearly exclusively of sulfuric acid hydrate (97%) with a small amount (3%) of 100μm grain water ice (Fig. 5). The model fit is only moderately good, and, critically, does not contain any of the magnesium sulfate brine required to cause a 2.07 μm absorption feature. We can only match the 2.07 μm feature by fixing the magnesium sulfate brine abundance to be about 30%. A spectral model with 34% sulfuric acid hydrate, 30% mag-
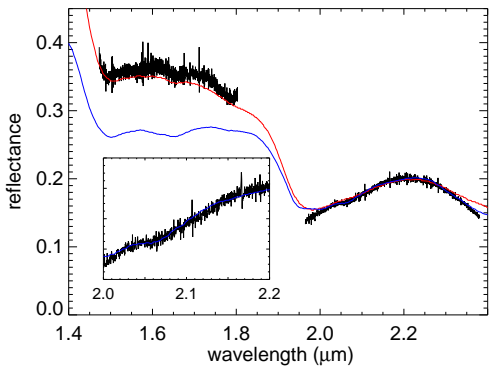
FIG. 5.— The spectrum of the low-latitude trailing hemisphere. The best linear spectral model consists almost entirely of hydrated sulfuric acid (red), but this model has no absorption at 2.07 μm absorption. A good fit to the 2.0-2.4 μm portion of the spectrum can be made by including nearly equal amounts of hydrated sulfuric acid and magnesium sulfate brine along with a dark neutral material (blue). While the fit of the 2.07 μm absorption feature is excellent, the fit to the continuum between 1.4 and 1.8 μm is poor. The inability to fit the full spectral region demonstrates the inadequacy of both the spectral library used and the general approach of linear spectral modeling.
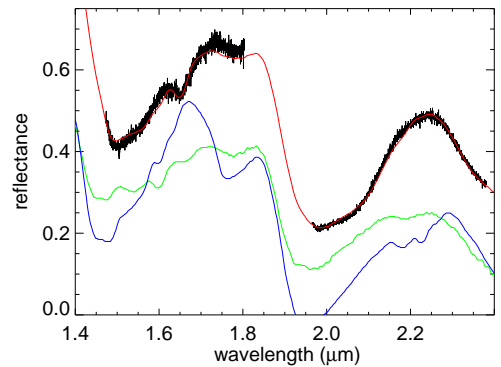

FIG. 6.— The low-latitude leading hemisphere spectrum of Europa compared to the best-fit linear model (red), which consists of 35.4% sulfuric acid hydrate, 18.2% hexahydrite, 17.9% mirabilite, 7.7% 100 μm grains of ice, and 20.6% 250 μm grains of ice. While the spectral fit appears good, careful inspection reveals that hexahydrite (green) and mirabilite (blue) have distinct absorption features that should be detectable in the spectrum. Hexahydrite and mirabilite both cause a small unobserved absorption feature at 1.6 μ, while mirabilite has a 2.18 μ absorption. The spectrum of the leading hemisphere is generally quite smooth with no clear spectral features other than those to to water ice.

nesium brine, and 36% dark neutral material provides an excellent fit to the 2 - 2.4 μm section of the spectrum – including fitting the location, width, and depth of the 2.07μm feature – but the fit to the continuum level of the 1.4 - 1.8 μm data is poor. The incorrect continuum fit to the 1.4 - 1.8 μm could be explained by at least one missing component in the spectral library. If the library contained a component that was mostly smooth across the two spectral bands but was more reflective than sulfuric acid hydrate at 1.5 μm, the algorithm would have selected this material to better match the spectrum. We discuss possibilities for such a material later.

The good spectral match of the 2.07 μm absorption feature to magnesium sulfate brines (and to epsomite) – along with the failed search to find any other material with a similar absorption feature – is compelling evidence that the new feature is indeed due to magnesium sulfate on the surface of Europa. While it is never possible to exhaust every other possibility, no other plausible species matches the spectrum.

5. SEARCH FOR ADDITIONAL SPECIES

In the analyses of Dalton and collaborators (Dalton 2007; Shirley et al. 2010; Dalton et al. 2012a,b), a general case is made that sulfate salts are ubiquitous on the surface of Europa but that the trailing hemisphere is dominated by radiolytically produced H_2SO_4. The mixing ratio of salt to acid is expected to increase from the trailing to the leading hemispheres. Again, however, the NIMS data show no distinctive absorption features of sulfate salts, but the overall spectral shape can be matched by various linear combinations of these salts.

The higher resolution spectra available here allow us to qualitatively examine this model and search for positive spectral evidence of these proposed materials. To study the region of the surface expected to be most salt-rich, we examine the spectrum of the leading hemisphere (Fig. 6). We attempt linear spectral modeling using the Dalton et al. library. Least-squares fitting finds what appears to be a moderately good solution with 35.4% sulfuric acid

hydrate, 18.2% hexahydrite, 17.9% mirabilite, 7.7% 100 μm grains of ice, and 20.6% 250 μm grains of ice.

At the spectral resolution of the NIMS data, this spectral fit would be considered excellent. The overall levels and shapes of the spectrum are nicely matched. Our spectra, however, show no evidence for many of the subtle absorption features that should be seen at the higher spectral resolution of our data. Hexahydrite and mirabilite both cause a small unobserved absorption feature at 1.6 μm, while mirabilite has a 2.18 μm absorption. Indeed, the spectrum of the leading hemisphere is generally quite smooth with no clear spectral features other than those due to water ice.

We conclude that we can find no evidence, on regional scales, of the specific salts modeled by Dalton et al. The apparent requirement for the presence of these species in the linear spectral modeling is simply a function of the limited number of species considered in the spectral library and the lack of distinct discriminating spectral features that can be seen at low resolution. While the spectral modeling appears to be indicating that some non-water ice component, non-sulfuric acid component is increasing in abundance from the trailing to the leading hemisphere, the current spectral libraries being used do not appear to contain the species that is causing this behavior.

6. DISCUSSION: THE SEA SALT HYPOTHESIS

The lack of any clear detection of sulfate salts on the leading hemisphere, coupled with the possible detection of magnesium sulfate salts on the trailing side is inconsistent with any of the hypotheses currently considered for the composition of the surface of Europa. Assuming that the 2.07 μm absorption is indeed due to magnesium sulfate, we consider an alternative hypothesis which could explain the observations.

The spatial correlation of magnesium sulfate with the radiolytically-produced sulfuric acid suggests the potential of an analogous magnesium radiation cycle. If magnesium is present on the surface of Europa as MgX, where

is X is an atomic or radical anion, bombardment by sulfur ions, in the presence of water, could yield a reaction such as

$$MgX_n + 4H_2O + S^+ \rightarrow MgSO_4 + 4H^+ + nX^-.$$
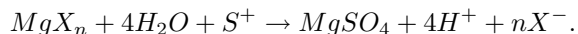
Such a cycle would suggest that MgX_n is a pre-radiation component of the surface of Europa. The presence of Na and K in the sputtered atmosphere of Europa (Brown & Hill 1996; Brown 2001) suggests that these cations should also be present, and that NaX and KX are likely also emplaced on the surface.

Sulfate has long been considered a plausible component of a Europa ocean based on both theoretical (Kargel 1991; Kargel et al. 2000) and experimental (Fanale et al. 2001) studies, though more detailed evolutionary models have suggested that sulfate could be much less abundant than initially expected (McKinnon & Zolensky 2003). In light of the lack of spectral evidence for sulfates on the leading hemisphere of Europa and keeping in mind the theoretical difficulties of high sulfate abundances, we explore alternative ocean chemistries. In the reduced ocean models of Zolotov (2008), for example, the most abundant cations are Na and K, the most abundant anion is chlorine. We thus consider the possibility here that the most abundant salts in Europa ocean brines are not sulfates, but are chlorides.

We consider the following conceptual model. Before irradiation, the non-water ice component of the surface of Europa is dominated by sodium and potassium chlorides, with magnesium chloride a more minor component. With sulfur bombardment, these chlorides are radiolytically converted to sulfates. Sodium and potassium sulfates are more easily sputtered than magnesium sulfates (McCord et al. 2001), so the trailing hemisphere shows an enhancement in magnesium sulfate above the initial magnesium mixing ratio. Nonetheless sodium and potassium sulfates should be present on the trailing side with the magnesium sulfates. Indeed, the spectrum of brines of sodium sulfate (McCord et al. 2002; Orlando et al. 2005; Dalton et al. 2005) have the general characteristic needed to better fit the continuum level on the trailing hemisphere.

The leading hemisphere should contain the spectral signature of NaCl and KCl salts (with a smaller amount of $MgCl_2$). NaCl, KCl, and $MgCl_2$ are all spectrally flat and, when hydrated, give distorted water bands with no distinct spectral features (see Fig. 4). Linear spectral models can easily be created which fit the leading hemisphere spectrum with these, rather than sulfate, salts, but we regard this fact more as a demonstration that linear spectral modeling, when faced with a spectrum that appears to be some sort of distorted water-ice spectrum, and when given a library of various distorted water-ice spectra, can nearly always find an adequate fit to the large-scale features of the spectrum. Evidence for the spectral detection of any salt materials on Europa should probably only be considered valid when a distinct spectral feature caused by the species can be specifically detected.

Because of their lack of distinct features in reflectance spectra, these chloride salts will prove much more difficult to spectrally rule out (or confirm) than the sulfate salts were. Like the detections of Na and K, it might prove more feasible to detect the presence of these compounds in gas phase once they have been sputtered from the surface, instead. Chlorine ions are detectable in the Io plasma torus (Küppers & Schneider 2000; Feldman et al. 2001) and atomic chlorine has been detected in Io's atmosphere (Feaga et al. 2004), but no search in the vicinity of Europa has been reported. NaCl and KCl vapor have been detected at millimeter wavelengths in circumstellar environments (Cernicharo & Guelin 1987). The feasibility of observations such as these should be studied to determine if there are possible ways to test the hypothesis that chloride salts dominate the non-irradiated non-water ice component of the surface of Europa.

7. CONCLUSION

Spatially resolved high resolution spectroscopy of the surface of Europa has allowed us to detect a previously unknown absorption feature at 2.07μm on the surface of Europa. This absorption feature is spatially correlated with other radiation products on the trailing hemisphere of Europa and is thus likely radiolytically produced. The only plausible spectral match to this absorption feature that we find is to the spectrum of $MgSO_4$ brine or that of the mineral epsomimte ($MgSO_4 \cdot 7H_2O$).

An examination of the spectrum of the less-irradiated leading hemisphere reveals that, while distorted water ice bands are indeed present at low latitudes, no evidence can be found that these distorted bands are caused by sulfate salts. Inclusion of these salts in models for the leading hemisphere spectrum results in distinct absorption features which are not observed in the high resolution spectra.

Based on the association of the potential $MgSO_4$ detection on the trailing side with other radiation products, we conclude that $MgSO_4$ is also an irradiation product, rather than a constituent of a Europa ocean brine. We hypothesize that, prior to irradiation, magnesium is primarily in the form of $MgCl_2$, and we predict that NaCl and KCl are even more abundant, and, in fact, dominate the non-ice component of the leading hemisphere. These salts are difficult to confirm spectroscopically in solid state form, but we suggest that detection of chlorine and NaCl in ionized or atomic state after sputtering might be possible.

REFERENCES

Anderson, J. D., Schubert, G., Jacobson, R. A., Lau, E. L., Moore, W. B., & Sjogren, W. L. 1998, Science, 281, 2019

Baldridge, A., Hook, S., Grove, C., & Rivera, G. 2009, Remote Sensing of the Environment, 113, 711

Brown, M. E. 2001, Icarus, 151, 190

Brown, M. E. & Hill, R. E. 1996, Nature, 380, 229

Calvin, W. M., Clark, R. N., Brown, R. H., & Spencer, J. R. 1995, Journal of Geophysical Research-Planets, 100, 19041

Carlson, R. W., Anderson, M. S., Johnson, R. E., Schulman, M. B., & Yavrouian, A. H. 2002, Icarus, 157, 456

Carlson, R. W., Anderson, M. S., Mehlman, R., & Johnson, R. E. 2005, Icarus, 177, 461

Carlson, R. W., Calvin, W. M., Dalton, J. B., Hansen, G. B., Hudson, R. L., Johnson, R. E., McCord, T. B., Moore, M. H., McKinnon, W. B., & Khurana, K. K. in Europa, ed. R. T. Pappalardo (Tucson, AZ: Univ. Arizona Press), 283

Carlson, R. W., Johnson, R. E., & Anderson, M. S. 1999, Science, 286, 97

Carlson, R. W., Weissman, P. R., Smythe, W. D., & Mahoney, J. C. 1992, Space Science Reviews, 60, 457

Cernicharo, J. & Guelin, M. 1987, A&A, 183, L10

Chyba, C. F. 2000, Nature, 403, 381

Clark, R., Swayze, G., Wise, R., Livo, E., Hoefen, T., Kokaly, R., & Sutley, S. 2007, USGS digitial spectral library splib06a: U.S. Geological Survey, Digital Data Series 231.

Dalton, J. B., & Pitman, K. M. 2012, Journal of Geophysical Research (Planets), 117, 09001

Dalton, J. B. 2007, Geophysical Research Letters, L21205, doi:10.1029/2007GL031497, 34

Dalton, J. B., Prieto-Ballesteros, O., Kargel, J. S., Jamieson, C. S., Jolivet, J., & Quinn, R. 2005, Icarus, 177, 472

Dalton, J. B., Shirley, J. H., & Kamp, L. W. 2012a, Journal of Geophysical Research-Planets, E03003, doi:10.1029/2011JE003909, 117

Dalton, J. I., Cassidy, T., Paranicas, C., Shirley, J., Prockter, L. M., & Kamp, L. 2012b, Planetary and Space Science, in press

Fanale, F. P., Li, Y. H., De Carlo, E., Farley, C., Sharma, S. K., Horton, K., & Granahan, J. C. 2001, Journal of Geophysical Research-Planets, 106, 14595

Feaga, L. M., McGrath, M. A., Feldman, P. D., & Strobel, D. F. 2004, ApJ, 610, 1191

Feldman, P. D., Ake, T. B., Berman, A. F., Moos, H. W., Sahnow, D. J., Strobel, D. F., Weaver, H. A., & Young, P. R. 2001, ApJ, 554, L123

Fink, U. & Sill, G. T. 1982, in IAU Colloq. 61: Comet Discoveries, Statistics, and Observational Selection, ed. L. L. Wilkening, 164–202

Grundy, W. M., Buratti, B. J., Cheng, A. F., Emery, J. P., Lunsford, A., McKinnon, W. B., Moore, J. M., Newman, S. F., Olkin, C. B., Reuter, D. C., Schenk, P. M., Spencer, J. R., Stern, S. A., Throop, H. B., & Weaver, H. A. 2007, Science, 318, 234

Hand, K. P., Chyba, C. F., Priscu, J. C., Carlson, R. W., Nealson, K. H., McKinnon, W. B., & Khurana, K. K. in Europa, ed. R. T. Pappalardo (Tucson, AZ: Univ. Arizona Press), 589

Hudson, R. L. & Moore, M. H. 2001, Journal of Geophysical Research-Planets, 106, 33275

Kargel, J. S. 1991, Icarus, 94, 368

Kargel, J. S., Kaye, J. Z., Head, J. W., Marion, G. M., Sassen, R., Crowley, J. K., Ballesteros, O. P., Grant, S. A., & Hogenboom, D. L. 2000, Icarus, 148, 226

Kivelson, M. G., Khurana, K. K., Russell, C. T., Volwerk, M., Walker, R. J., & Zimmer, C. 2000, Science, 289, 1340

Küppers, M. & Schneider, N. M. 2000, Geophys. Res. Lett., 27, 513

Lane, A. L., Nelson, R. M., & Matson, D. L. 1981, Nature, 292, 38

Larkin, J. E., Quirrenbach, A., Krabbe, A., Aliado, T., Barczys, M., Brims, G., Canfield, J., Gasaway, T., LaFreniere, D., Magone, N., Skulason, G., Spencer, M., Sprayberry, D., & Weiss, J. 2003, Instrument Design and Performance for Optical/Infrared Ground-Based Telescopes, Pts 1-3, 4841, 1600

McCord, T. B., Hansen, G. B., Combe, J. P., & Hayne, P. 2010, Icarus, 209, 639

McCord, T. B., Hansen, G. B., Fanale, F. P., Carlson, R. W., Matson, D. L., Johnson, T. V., Smythe, W. D., Crowley, J. K., Martin, P. D., Ocampo, A., Hibbitts, C. A., Granahan, J. C., & Team, N. 1998, Science, 280, 1242

McCord, T. B., Hansen, G. B., & Hibbitts, C. A. 2001, Science, 292, 1523

McCord, T. B., Hansen, G. B., Matson, D. L., Johnson, T. V., Crowley, J. K., Fanale, F. P., Carlson, R. W., Smythe, W. D., Martin, P. D., Hibbitts, C. A., Granahan, J. C., & Ocampo, A. 1999, Journal of Geophysical Research-Planets, 104, 11827

McCord, T. B., Teeter, G., Hansen, G. B., Sieger, M. T., & Orlando, T. M. 2002, Journal of Geophysical Research-Planets, 5004, 10.1029/2000JE001453, 107

McEwen, A. S. 1986, J. Geophys. Res., 91, 8077

McKinnon, W. B. & Zolensky, M. E. 2003, Astrobiology, 3, 879

Moore, M. H., Hudson, R. L., & Carlson, R. W. 2007, Icarus, 189, 409

Orlando, T. M., McCord, T. B., & Grieves, G. A. 2005, Icarus, 177, 528

Paranicas, C., Carlson, R. W., & Johnson, R. E. 2001, Geophysical Research Letters, 28, 673

Paranicas, C., Mauk, B. H., Ratliff, J. M., Cohen, C., & Johnson, R. E. 2002, Geophysical Research Letters, 29, 18

Shirley, J. H., Dalton, J. B., Prockter, L. M., & Kamp, L. W. 2010, Icarus, 210, 358

Spencer, J. R., Grundy, W. M., Dumas, C., Carlson, R. W., McCord, T. B., Hansen, G. B., & Terrile, R. J. 2006, Icarus, 182, 202

Strazzulla, G., Baratta, G. A., Leto, G., & Gomis, O. 2007, Icarus, 192, 623

Zimmer, C., Khurana, K. K., & Kivelson, M. G. 2000, Icarus, 147, 329

Zolotov, M. Y. 2008, in Lunar and Planetary Inst. Technical Report, Vol. 39, Lunar and Planetary Institute Science Conference Abstracts, 2349

TABLE 1

Time (UT)	target	spectra setting	int. time (sec)	airmass	Europa lon. (deg)	comments
18 Sep 2011						
09:10	Europa, west	Kbb	900	1.80	41	
09:26	Europa, east	Kbb	900	1.64	43	
09:44	sky	Kbb	450	1.50		
10:07	NLTT7066	Kbb	100	1.37		telluric calibrator
10:09	NLTT7066	Kbb	100	1.35		telluric calibrator
10:12	NLTT7066	Hbb	50	1.34		telluric calibrator
10:14	NLTT7066	Hbb	50	1.33		telluric calibrator
10:22	Europa, west	Hbb	450	1.29	47	
10:31	Europa, east	Hbb	450	1.25	48	
10:40	sky	Hbb	450	1.22		
19 Sep 2011						
08:48	HD9986	Kbb	20	1.50		telluric calibrator
08:49	HD9986	Kbb	20	1.49		telluric calibrator
08:53	NLTT7066	Kbb	20	1.91		transmission calibrator
08:54	NLTT7066	Kbb	20	1.90		transmission calibrator
09:05	Europa, west	Kbb	900	1.81	143	
09:21	sky	Kbb	900	1.65		
09:37	Europa, east	Kbb	900	1.51	145	
09:57	NLTT7066	Kbb	20	1.40		transmission calibrator
09:58	NLTT7066	Kbb	20	1.39		transmission calibrator
10:05	HD9986	Hbb	20	1.16		telluric & transmission calibrator
10:06	HD9986	Hbb	20	1.16		
10:48	Europa, west	Hbb	450	1.18	150	
10:57	sky	Hbb	450	1.15		
11:06	Europa, east	Hbb	450	1.13	151	
13:58	HD9986	Kbb	20	1.12		telluric calibrator star
13:59	HD9986	Kbb	20	1.13		telluric calibrator star
14:04	Europa, west	Kbb	900	1.04	164	
14:20	sky	Kbb	900	1.06		
14:37	Europa, east	Kbb	900	1.09	166	
14:58	HD9986	Hbb	20	1.33		telluric & transmission calibrator
14:59	HD9986	Hbb	20	1.34		
15:05	Europa, west	Hbb	450	1.16		
15:13	sky	Hbb	450	1.18		
15:22	Europa, east	Hbb	450	1.21		
20 Sep 2011						
09:09	Europa, west	Kbb	900	1.72	244	
09:26	sky	Kbb	900	1.57		
09:43	Europa, east	Kbb	900	1.45	247	
10:03	NLTT7066	Kbb	20	1.35		telluric calibrator star
10:04	NLTT7066	Kbb	20	1.34		telluric calibrator star
10:19	HD9986	Hbb	20	1.12		telluric calibrator star
10:21	HD9986	Hbb	20	1.11		telluric calibrator star
10:33	Europa, west	Hbb	450	1.22	250	
10:42	sky	Hbb	450	1.18		
10:51	Europa, east	Hbb	450	1.16	252	